Supplementary Information (SI) for Journal of Materials Chemistry C.
This journal is © The Royal Society of Chemistry 2025

Electronic Supporting Information Available

Efficient NIR-OLEDs based on color-purity near-infrared (NIR) *tris*-/*bis*-heteroleptic iridium(III) complexes with single color-responsible ligand

Youquan Chen,[#a] Siyu Hou,[#a] Yan Zhang,[a] Mingfeng Tan,[a] Xingqiang Lü,*[a] Guorui Fu*[a] and Wai-Yeung Wong*[b]

Supporting information

Materials and characterization

All reagents were received from Sigma Aldrich and used without further purification. All solvents unless otherwise stated were degassed and stored over 3 Å activated molecular sieves prior to use. All manipulations of air and water sensitive compounds were carried out under dry N_2 using the standard Schlenk line techniques.

Elemental analysis (EA) was performed on a Perkin-Elmer 240C elemental analyzer. Fourier Transform Infrared (FT-IR) spectra were recorded on a Nicolet Nagna-IR 550 spectrophotometer in the region 4000-400 cm^{-1} using KBr pellets. ^1H NMR spectra were recorded on a JEOL EX 400 spectrometer with $SiMe_4$ as internal standard in $CDCl_3$ or DMSO-d_6 at room temperature. Electro-spray ionization mass spectrometry (ESI-MS) was performed on a Finnigan LCQ^{DECA} XP HPLC-MS_n mass spectrometer with a mass to charge (*m/z*) range of 4000 using a standard electro-spray ion source and CH_2Cl_2 as the solvent. Electronic absorption spectra in the UV-visible-NIR region were recorded with a Cary 300 UV spectrophotometer.

Visible or NIR emission and excitation spectra were collected by a combined fluorescence lifetime and steady-state spectrometer (FLS-980, Edinburgh) with a 450 W Xe lamp. Excited-state decay times were obtained by the same spectrometer but with a μF900 Xe lamp. The quantum yield (Φ_{PL}) in solution was measured with free-base tetraphenylporphyrin (Φ_r = 0.13 in toluene solution at 298 K) as the standard.[1] The solution was degassed by three freeze-pump-thaw circles. The following equation 1 was used to calculate the quantum yields:

$$\Phi_s = \Phi_r \times [(n_s^2 \times A_r \times I_s)/(n_r^2 \times A_s \times I_r)] \quad (1)$$

where Φ_s is the quantum yield of the sample, Φ_r is the quantum yield of the reference, n_s is the refractive index of the sample, n_r is the refractive index of the reference, A_s and A_r are the absorbance of the sample and the reference at the wavelength of excitation (355 nm), respectively, and the I_s and I_r are the integrated areas of emission bands of the sample and the reference from 600 to 900 nm, which were recorded by a red photomultiplier tube (PMT) detector. Thermal properties were characterized using thermogravimetric (TG) analyses on a NETZSCH TG 209 instrument under a flow of nitrogen at a heating rate of 10 °C/min.

Synthesis of the HC^N ligand Hdpbq (Hdpbq = 1-(benzo[*b*]-thiophen-2-yl)-isoquinoline)

The HC^N ligand Hdpbq was synthesized from the well-established procedure from the literature [2]. A mixture of 2,3-naphthalenediamine (1.000 g, 6.33 mmol), oxalic acid (0.018 g, 0.2 mmol) and DMSO (20 mL) in a 50 mL round-bottomed flask was add benzil (1.329g, 6.33 mmol) and the resulting mixture was stirred at room temperature for 3 h. Then, H_2O (20 mL) was added to the reaction mixture, and allowed to stand at room temperature for 1 hours.

During this time, the yellow powder formed which were collected by filtration and dried. Then, the powder was recrystallized by absolute ethanol to afford the yellow needle-like polycrystalline solid product. For **Hdpbq**: Yield: 1.80 g (86%). Calcd. for $C_{24}H_{16}N_2$: C, 86.72; H, 4.85; N, 8.43. Found: C, 86.75; H, 4.86; N, 8.39%. ^{1}H NMR ($CDCl_3$, 400 MHz): δ(ppm) 8.78 (s, 2H, -Ph), 8.15 (q, 2H, -Ph), 7.59 (m, 6H, -Ph), 7.40 (m, 6H, -Ph).

Synthesis of the HC'^N' ligand Hiqbt (Hiqbt = 1-(benzo[*b*]-thiophen-2-yl)-isoquinoline)

The HC'^N' ligand **Hiqbt** was synthesized from the improved Suzuki coupling reaction of 2-chloro-isoquinoline[3] (instead of 2-bromo-isoquinoline[4]) with benzo[*b*]thien-2-yl boronic acid. A mixture of 2-chloro-isoquinoline (0.653 g, 4.0 mmol) and benzo[*b*]thien-2-y boronic acid (0.713 g, 4.0 mmol) was dissolved into absolute mixed solvents of toluene-EtOH (60 mL; v/v = 2:1) under a N_2 atmosphere. Then an aqueous solution (20 mL) of Na_2CO_3 (2 M) was added, and the mixture was degassed by a N_2 flow. Anhydrous $Pd(PPh_3)_4$ (0.190 g, 0.2 mmol; 5 mol%) was added to the reaction mixture which was then heated at 85 °C for 48 h. The complete consumption of reagents was monitored by thin-layer chromatography (Hexane/AcOEt, v/v = 9:1). After cooling to room temperature, the organic phase was washed with brine and extracted with absolute CH_2Cl_2 (3×20 mL) three times. The combined organic phase was dried over anhydrous Na_2SO_4, and further purified with flash-column chromatography on silica gel (Hexane/AcOEt, v/v = 9:1), affording an off-white solid. For **Hiqbt**: Yield: 0.762 g (73%). Calcd for $C_{17}H_{11}NS$: C, 78.13; H, 4.24; N, 5.36%. Found: C, 78.05; H, 4.36; N, 5.29%. ^{1}H NMR (400 MHz, DMSO-d_6): δ(ppm) 8.70 (d, 1H, -Py), 8.61 (d, 1H, -Ph), 8.19 (s, 1H, -Th), 8.11 (d, 1H, -Ph), 8.06 (m, 1H, -Ph), 8.02 (m, 1H, -Py), 7.89 (m, 2H, -Ph), 7.82 (t, 1H, -Ph), 7.46 (m, 2H, -Ph).

Synthesis of the N''^OH ancillary ligand Hpbi (Hpbi = 2-(1*H*-benzo[*b*]imidazol-2-yl)-phenol)

The N''^OH-ancillary π-donor ligand **Hpbi** was synthesized according to an improved synthetic procedure as the literature.[5] To a solution of $NaHSO_3$ (1.040 g, 10 mmol) in absolute DMF (20 mL), salicylaldehyde (1.122 g, 1.066 mL, 10.0 mmol) was added slowly and the resulting mixture was continuously stirred at room temperature for 0.5 h. subsequently, 1,2-diaminobenzene (0.440 g, 2 mmol) was added, and the mixture's colour was changed from yellow to reddish-brown during reaction under refluxing at 80 °C for 12 h. After cooling to room temperature, excess D. I. water (100 mL) was poured into the mixture, and the white suspension was filtrated, affording to an off-white crude product. The crude powder was further re-crystallized with absolute EtOH to get off-white polycrystalline. For the **Hpbi**: Yield: 1.682 g (80%). Calc. for $C_{13}H_{10}N_2O$: C, 74.27; H, 4.79; N, 13.33%. Found: C, 74.21; H, 4.86; N, 13.30%. ^{1}H NMR (400 MHz, DMSO-d_6): δ (ppm) 13.18 (2H, -NH/-OH), 8.06 (m, 1H, -Ph), 7.67 (m, 2H, -Ph), 7.39 (t, 1H, -Ph), 7.29 (d, 2H, -Ph), 7.04 (m, 2H, -Ph).

X-ray crystallography

Single crystals of the Ir(III)-complex **2**·MeOH·H_2O ([Ir(dpbq)(iqbt)(pbi)]·MeOH·H_2O) of suitable dimensions were mounted onto thin glass fibers. All the intensity data were collected on a Bruker SMART CCD diffractometer (Ga-Kα radiation and λ = 1.34139 Å) in Φ and scan modes. Structures were solved by Direct methods followed by difference Fourier syntheses, and then refined by full-matrix least-squares techniques against F^2 using SHELXTL.[6] All other non-hydrogen atoms were refined with anisotropic thermal parameters. Absorption corrections were applied using SADABS.[7] All hydrogen atoms were placed in calculated

positions and refined isotropically using a riding model. Crystallographic data and selected atomic distances and bond angles are presented in **Tables S1-2**, respectively. CCDC reference number 2374166 is for the Ir(III)-complex **2**·MeOH·H_2O ([Ir(dpbq)(iqbt)(pbi)]·MeOH·H_2O).

Electronic structure calculations

To gain further insight into the photophysical and electrochemical characteristics of the Ir(III)-complexes **1**-**2**, theoretical studies on their electronic structures were carried out by using density functional theory (DFT) and time-dependent DFT (TD-DFT) methods. Each of their molecular structures was optimized at the ground state (S_0) in the gas phase. TD-DFT calculations using the B3LYP functional were then performed on the basis of the structural optimized geometries.[8] The 6-31G (d,p) basis set was applied for C, H, N, O atoms, while effective core potentials employed for Ir atom were based on a LanL2DZ basis set.[9-10] The energies of the excited states of the Ir(III)-complex were computed by TD-DFT based on all the ground-state (S_0) geometries. Calculations of the permanent dipole moments (μ) of the different emitters were performed by DFT single point energy calculations using the hybrid functional B3LYP with the def2tzvp basis set based on the corresponding optimized S_0 and T_1 states. The inter fragment charge transfer (IFCT)[11] in the electronic excitation process were analyzed by the Ros and Schuit method[12] (C-squared population analysis method, SCPA) in the Multiwfn 3.8 program.[13] All calculations were carried out with Gaussian 09, Revision D.01 software package.[14] The electron density diagrams of the molecular orbitals were obtained with the crystal structure.

Cyclic voltammetry (CV) measurement

Electro-chemical measurements were made using a Princeton Applied Research model 2273A potentiostat at a scan rate of 100 mV/s. A conventional three-electrode configuration consisting of a glassy carbon working electrode, a Pt-sheet counter electrode, and a Pt wire reference electrode was used. The supporting electrolyte was 0.1 M tetrabutylammonium tetrafluoroborate ($[Bu_4N]BF_4$) in anhydrous MeCN. Ferrocene was added as a calibrant after each set of measurements, and all potentials reported are quoted with reference to the Fc^+/Fc couple. The oxidation (E_{ox}) and reduction (E_{red}) potentials were used to determine the HOMO and LUMO energy levels using Equations (2) and (3),[15] respectively,

$$E_{HOMO} = -[(E_{ox}^{on} - E_{1/2,ferrocene})eV + 4.8]\ eV \quad (2)$$

$$E_g^{opt} = 1240/\lambda_{edge} \quad (3)$$

$$E_g = E_{LUMO} - E_{HOMO} \quad (4)$$

where E_{ox}^{on} is the recorded onset oxidation potential and $E_{1/2,ferrocene}$ is internal standard ferrocene Oxidation half potential. E_g^{opt} is the energy band gap estimated from the low-energy edge of the absorption spectra from the samples。The HOMO and LUMO energy levels for the other used materials were obtained from the literatures.[16]

Fabrication and determination of the solution-processed color-purity NIR-OLEDs-1/2 doped with $[Ir(dpbq)_2(pbi)]$ (1) or [Ir(dpbq)(iqbt)(pbi)] (2)

Each of the color-purity **NIR-OLEDs-1/2** was fabricated on ITO (Indium tin oxide) coated glass substrates with a sheet resistance of 20 Ω per square. Patterned ITO coated glass substrates

were washed with acetone, detergent, D. I. water and isopropanol in an ultrasonic bath. After being exposed under oxygen plasma for 20 min, PEDOT:PSS from water solution was spin-coated (at 4800 rpm) on the substrate followed by drying in a vacuum oven at 130 °C for 30 min, giving a film of 40 nm in thickness. The 1,2-dichloroethane solution (10 mg/mL) of the mixture (65:30:*x*; wt%; *x* = 2, 5 or 8) of PVK, OXD7 and one of Ir(III)-complexes (**1/2**; $[(dpbq)_2(pbi)]$ (**1**) and [(dpbq)(iqbt)(pbi)] (**2**)) as the emitting layer (EML), was prepared under an N_2 atmosphere and spin-coated (at 1500 rpm) on the PEDOT:PSS layer with a thickness of 60 nm. Finally, a thin layer (1 nm) of LiF followed by Al capping layer (120 nm) was deposited onto the substrate under vacuum (5×10^{-6} Pa). Current density-voltage (*J*-*V*) characteristics were collected using a Keithley 4200 semiconductor characterization system, and optical power was recorded on a Newport 1936-C power meter coupled to a calibrated Newport 918D-UV-OD3 detector with a spectral response. EL spectra were collected with a Jobin Yvon FluoroMax-3 spectrophotometer. All measurements were carried out in air at room temperature with encapsulation.

References

1 J. H. Palmer, A. C. Durrell, Z. Gross, J. R. Winkler and H. B. Gray, *J. Am. Chem. Soc.*, 2010, **132**, 9230-9231.

2 J. H. Guo, J. Zhou, G. R. Fu, Y. N. He, W. T. Li and X. Q. Lü, *Inorg. Chem. Commun.,* 2019, **101**, 69-73.

3 G. R. Fu, H. Zheng, Y. N. He, W. T. Li, X.Q. Lü and H. S. He, *J. Mater. Chem. C*, 2018, **6**, 10589-10596.

4 S. Kesarkar, W. Mróz, M. Penconi, M. Pasini, S. Destri, M.Cazzaniga, D. Ceresoli, P. R. Mussini, C. Baldoli, U. Giovanella and A. Bossi, *Angew. Chem. Int. Ed.*, 2016, **55**, 2714-2718.

5 M. Martínez-Alonso, N. Busto, L. D. Aguirre, L. Berlanga, M. C. Carrión, J. V. Cuevas, A. M. Rodríguez, A. Carbayo, B. R. Manzano, E. Ortí, F. A. Jalón, B. García and G. Espino, *Chem. Eur. J.* 2018, **24**, 17523-17537.

6 G. M. Sheldrick, SHELXL-97: Program for crystal structure refinement, Göttingen, Germany, 1997.

7 G. M. Sheldrick, *SADABS*, University of Göttingen, Germany, 1997.

8 (a) A. D. Becke, *J. Chem. Phys*. 1993, **98**, 5648-5652; (b) C. Lee, W. Y. and R. G. Parr, *Phys. Rev. B: Condens. Matter Mater. Phys*. 1988, **37**, 785-789.

9 W. R. Wadt and P. J. Hay, *J. Chem. Phys*., 1985, **82**, 284-298.

10 P. J. Hay and W. R. Wadt, *J. Chem. Phys*., 1985, **82**, 299-310.

11 T. Lu, Multiwfn Manual, version 3.6 (dev), Section 3.21.1 and 3.21.8, available at http://sobereva.com/multiwfn.

12 P. Ros and G. C. A. Schuit, *Theor. Chim. Acta*., 1966, **4**, 44-63.

13 T. Lu and F. W. Chen, *J. Comput. Chem*., 2012, **33**, 580-592.

14 M. J. Frisch, G. W. Trucks, H. B. Schlegel, G. E. Scuseria, M. A. Robb, J. R. Cheeseman, G. Scalmani, V. Barone, B. Mennucci, G. A. Petersson, H. Nakatsuji, M. Caricato, X. Li, H. P. Hratchian, A. F. Izmaylov, J. Bloino, G. Zheng, J. L. Sonnenberg, M. Hada, M. Ehara, K. Toyota, R. Fukuda, J. Hasegawa, M. Ishida, T. Nakajima, Y. Honda, O. Kitao, H. Nakai, T. Vreven, J. A. Montgomery, Jr., J. E. Peralta, F. Ogliaro, M. Bearpark, J. J. Heyd, E. Brothers, K. N. Kudin, V. N. Staroverov, R. Kobayashi, J. Normand, K. Raghavachari, A. Rendell, J. C. Burant, S. S. Iyengar,

J. Tomasi, M. Cossi, N. Rega, J. M. Millam, M. Klene, J. E. Knox, J. B. Cross, V. Bakken, C. Adamo, J. Jaramillo, R. Gomperts, R. E. Stratmann, O. Yazyev, A. J. Austin, R. Cammi, C. Pomelli, J. W. Ochterski, R. L. Martin, K. Morokuma, V. G. Zakrzewski, G. A. Voth, P. Salvador, J. J. Dannenberg, S. Dapprich, A. D. Daniels, ö. Farkas, J. B. Foresman, J. V. Ortiz, J. Cioslowski, D. J. Fox, Gaussian 09, Revision D.01, Gaussian, Inc., Wallingford CT, 2009.

15 H. Y. Chen, C. T. Chen and C. T. Chen, *Macromolecules,* 2010, **43**, 3613-3623.

16 E. Zysman-Colman, S. S. Ghosh, G. Xie, S. Varghese, M. Chowdhury, N. Sharma, D. B. Cordes, A. M. Z. Slawin and I. D. W. Samuel, *ACS Appl. Mater. & Interfaces,* 2016, **8**, 9247-9253.

Table S1 Crystal data and structure refinement for the Ir(III)-complex **2·$CH_3OH·H_2O$**

Compound	**2·$CH_3OH·H_2O$**
formula	$C_{55}H_{40}IrN_5O_3S$
fw	1043.18
cryst syst	monoclinic
space group	$P2_1/c$
a, Å	12.6352(17)
b, Å	17.5350(16)
c, Å	20.874(3)
α, deg	90
β, deg	101.830(7)
γ, deg	90
V, Å3	4526.5(10)
Z	4
ρ, g·cm-3	1.531
size, mm	0.28× 0.26 × 0.19
μ(Mo-Kα), mm^{-1}	4.334
data/restraints/parameters	8671/1/591
quality-of-fit indicator	1.046
No. observed reflections	39044
final R indices [I> 2σ(I)]	0.0428
	0.1162
R indices (all data)	0.0486
	0.1232

Table S2 The relevant bond lengths (Å) and bond angles (°) for the Ir(III)-complex **2·$CH_3OH·H_2O$**

Complex	**2·$CH_3OH·H_2O$**
Ir(1)-C(1)	1.974(5)
Ir(1)-N(1)	2.038(4)
Ir(1)-C(25)	1.983(5)
Ir(1)-N(3)	2.037(4)
Ir(1)-N(4)	2.154(4)
Ir(1)-O(1)	2.140(3)
C(1)-Ir(1)-N(1)	79.83(17)
C(1)-Ir(1)-N(3)	98.14(17)
C(1)-Ir(1)-C(25)	88.63(18)
C(1)-Ir(1)-O(1)	86.51(15)
C(1)-Ir(1)-N(4)	168.30(16)

Table S3 Frontier orbital energy and electron density distribution for [Ir(dpbq)$_2$(pbi)] (**1**) and [Ir(dpbq)(iqbt)(pbi)] (**2**) on the basis of their optimized S_0 geometries

Complex	MO	Contribution of metal d_π orbitals and π orbitals of ligand to MOs (%)			
		Ir	**dpbq-1**	**dpbq-2**	**pbi**
1	LUMO+2	1.70	68.04	29.05	1.21
	LUMO+1	3.79	92.52	3.01	0.68
	LUMO	3.17	3.03	93.02	0.78
	HOMO	13.00	7.22	3.11	76.67
	HOMO-1	36.06	25.97	26.47	11.49
	HOMO-2	7.43	65.74	23.63	3.21
		Ir	**dpbq**	**iqbt**	**pbi**
2	LUMO+2	1.00	94.85	0.91	3.24
	LUMO+1	5.34	0.55	92.72	1.40
	LUMO	3.64	95.07	0.43	0.86
	HOMO	22.68	8.01	39.64	29.68
	HOMO-1	13.98	5.94	22.12	57.96
	HOMO-2	5.97	78.79	12.68	2.56

Table S4 Frontier orbital energy and electron density distribution for [Ir(dpbq)$_2$(pbi)] (**1**) and [Ir(dpbq)(iqbt)(pbi)] (**2**) on the basis of their optimized T_1 geometries

Complex	MO	Contribution of metal d_π orbitals and π orbitals of ligand to MOs (%)			
		Ir	**dpbq-1**	**dpbq-2**	**pbi**
1	LUMO+2	1.62	63.01	34.54	0.82
	LUMO+1	3.09	0.61	95.56	0.74
	LUMO	4.32	94.25	0.72	0.72
	HOMO	13.18	9.20	3.26	74.36
	HOMO-1	27.16	41.68	16.51	14.65
	HOMO-2	13.38	68.18	16.96	1.49
		Ir	**dpbq**	**iqbt**	**pbi**
2	LUMO+2	1.01	93.76	1.25	3.98
	LUMO+1	5.19	0.78	92.68	1.36
	LUMO	5.00	93.23	0.60	1.17
	HOMO	20.75	7.44	37.85	33.97
	HOMO-1	16.85	16.55	22.13	44.46
	HOMO-2	2.34	74.70	10.24	12.72

Table S5 The calculated orbital transition analyses for [Ir(dpbq)$_2$(pbi)] (**1**) and [Ir(dpbq)(iqbt)(pbi)] (**2**) by TD-DFT calculations with the IFCT analyses at the B3LYP level

Comp	State	λ (nm)	E (eV)	Oscillator (f)	transition (contrib.%)	Assignment (%)
1	$S_0 \rightarrow S_1$	663	1.87	0.0182	H $\rightarrow$ L (98.29)	^{1}ILCT(3.71)/^{1}MLCT(12.59)/^{1}LLCT(80.53)
	$S_0 \rightarrow S_2$	643	1.93	0.0042	H $\rightarrow$ L+1 (96.40)	^{1}ILCT(7.30)/^{1}MLCT(12.51)/^{1}LLCT(76.40)
	$S_0 \rightarrow S_3$	601	2.06	0.0177	H-1 $\rightarrow$ L (94.64)	^{1}ILCT(25.50)/^{1}MLCT(34.92)/^{1}LLCT(36.41)
	$S_0 \rightarrow T_1$	763	1.63	0.0000	H-2 $\rightarrow$ L+1 (38.93) H-3 $\rightarrow$ L (18.94) H-1 $\rightarrow$ L (14.19)	^{3}ILCT(43.53)/^{3}MLCT(11.58)/^{3}LLCT(41.37)
	$T_1 \rightarrow S_0$	1164	1.07	0.0000	H-1 $\rightarrow$ L (42.15) H-2 $\rightarrow$ L (51.47)	^{3}ILCT(84.42)/^{3}MLCT(6.87)/^{3}LLCT(4.38)
2	$S_0 \rightarrow S_1$	652	1.90	0.0226	H $\rightarrow$ L (98.07)	^{1}ILCT(8.04)/^{1}MLCT(21.85)/^{1}LLCT(66.47)
	$S_0 \rightarrow S_2$	610	2.03	0.0049	H-1 $\rightarrow$ L (98.00)	^{1}ILCT(6.24)/^{1}MLCT(13.47)/^{1}LLCT(76.65)
	$S_0 \rightarrow S_3$	522	2.38	0.0669	H $\rightarrow$ L +1(95.72)	^{1}ILCT(37.21)/^{1}MLCT(21.47)/^{1}LLCT(35.99)
	$S_0 \rightarrow T_1$	755	1.64	0.0000	H-1 $\rightarrow$ L (15.59) H-2 $\rightarrow$ L (66.79)	^{3}ILCT(78.81)/^{3}MLCT(11.66)/^{3}LLCT(5.89)
	$T_1 \rightarrow S_0$	1171	1.06	0.0000	H-1 $\rightarrow$ L (29.92) H-2 $\rightarrow$ L (65.73)	^{3}ILCT(80.25)/^{3}MLCT(10.66)/^{3}LLCT(4.09)

Figure S1. The ^{1}H NMR spectra of the HC^N ligand **Hdpbq** in $CDCl_3$ at room temperature.

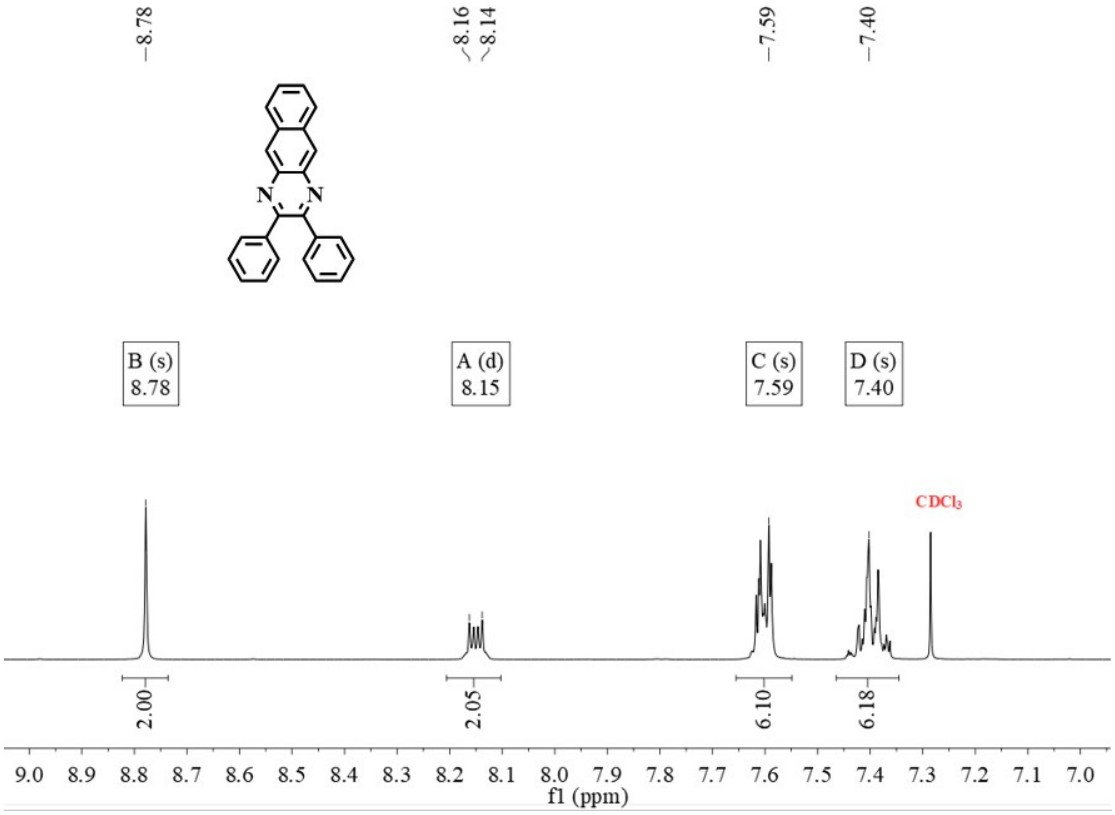

Figure S2. The ^{1}H NMR spectrum of the HC'^N' ligand **Hiqbt** in DMSO-d_6 at room temperature.

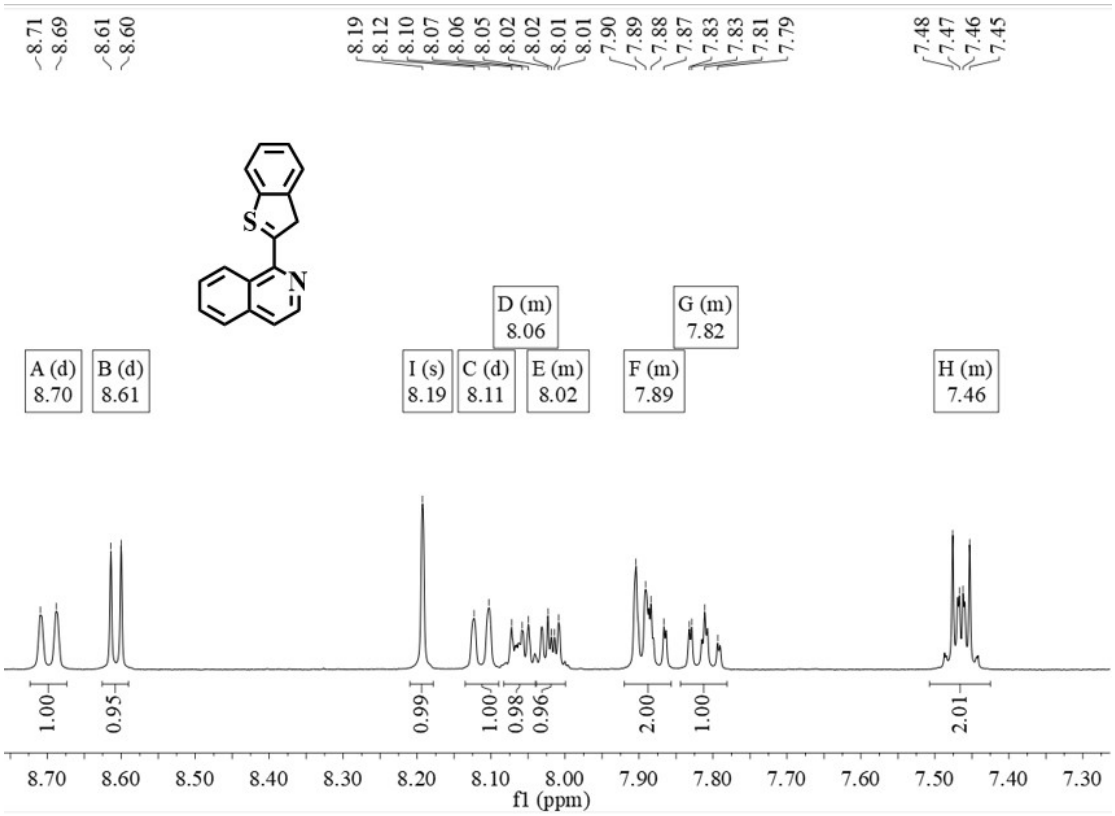

Figure S3. The ^{1}H NMR spectrum of the N''^OH ancillary ligand **Hpbi** in DMSO-d_6 at room temperature.

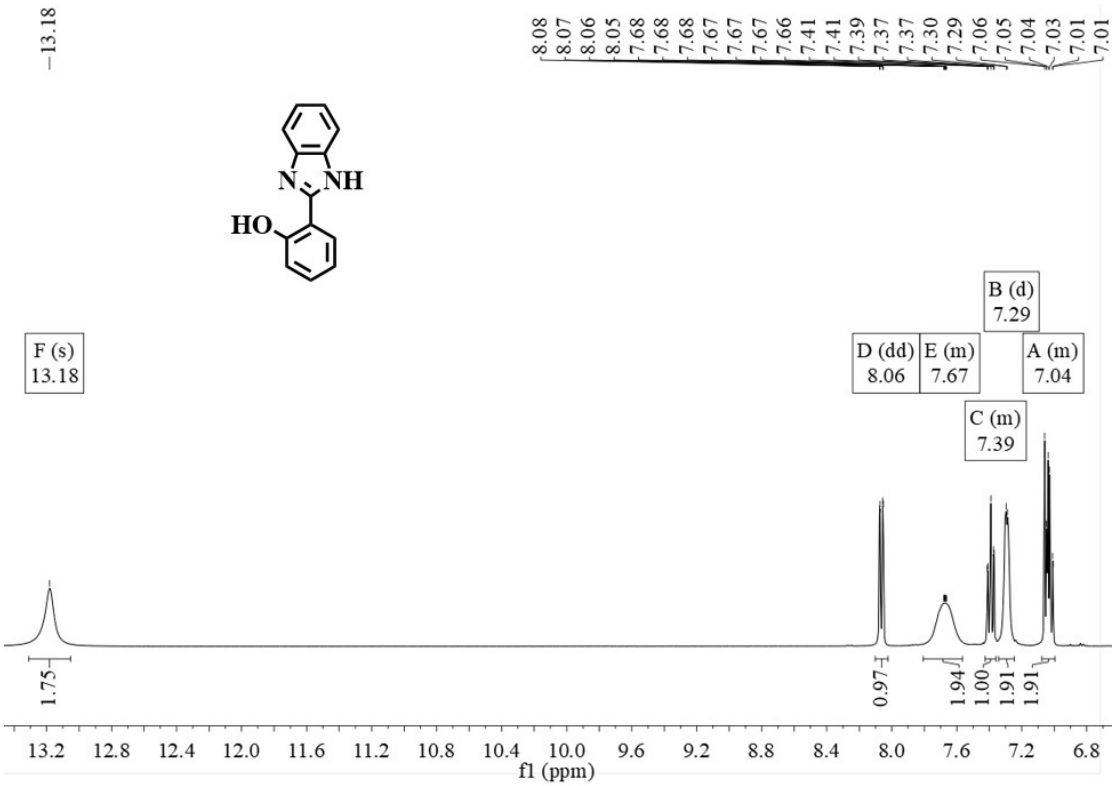

Figure S4. The ^{1}H NMR spectrum of $[Ir(dpbq)_2(pbi)]$ (**1**) in $CDCl_3$ at room temperature.

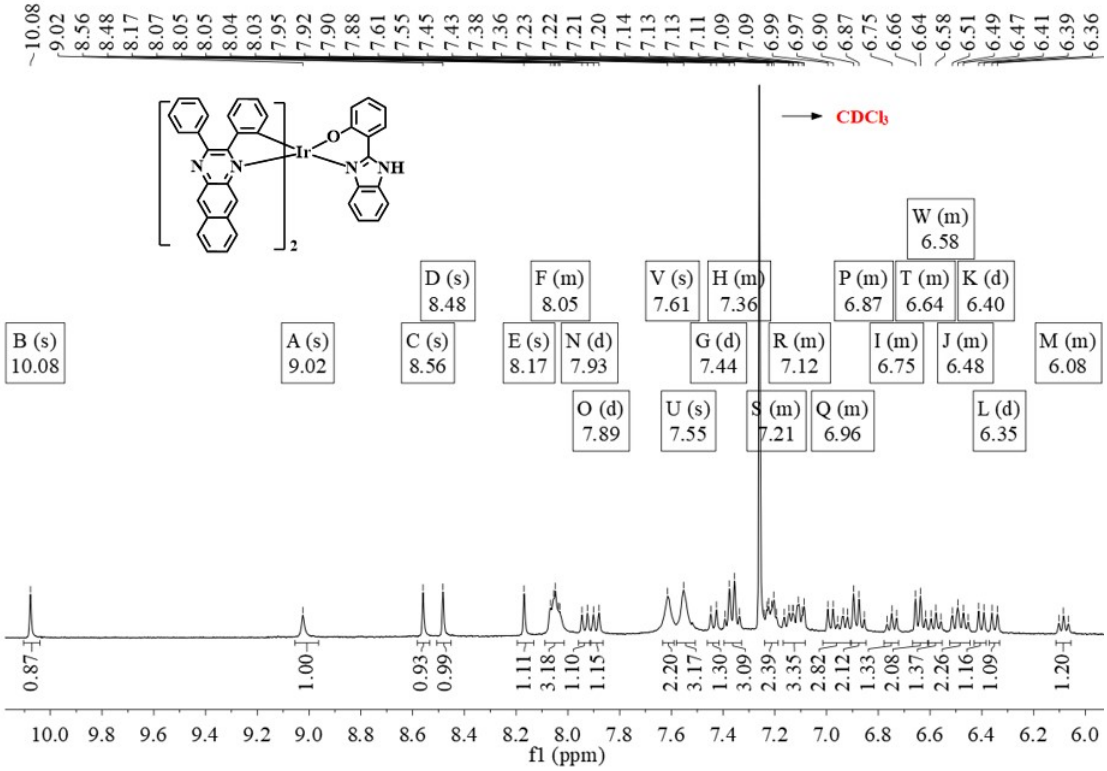

Figure S5. The ^{1}H NMR spectrum of [Ir(dpbq)(iqbt)(pbi)] (**2**) in $CDCl_3$ at room temperature.

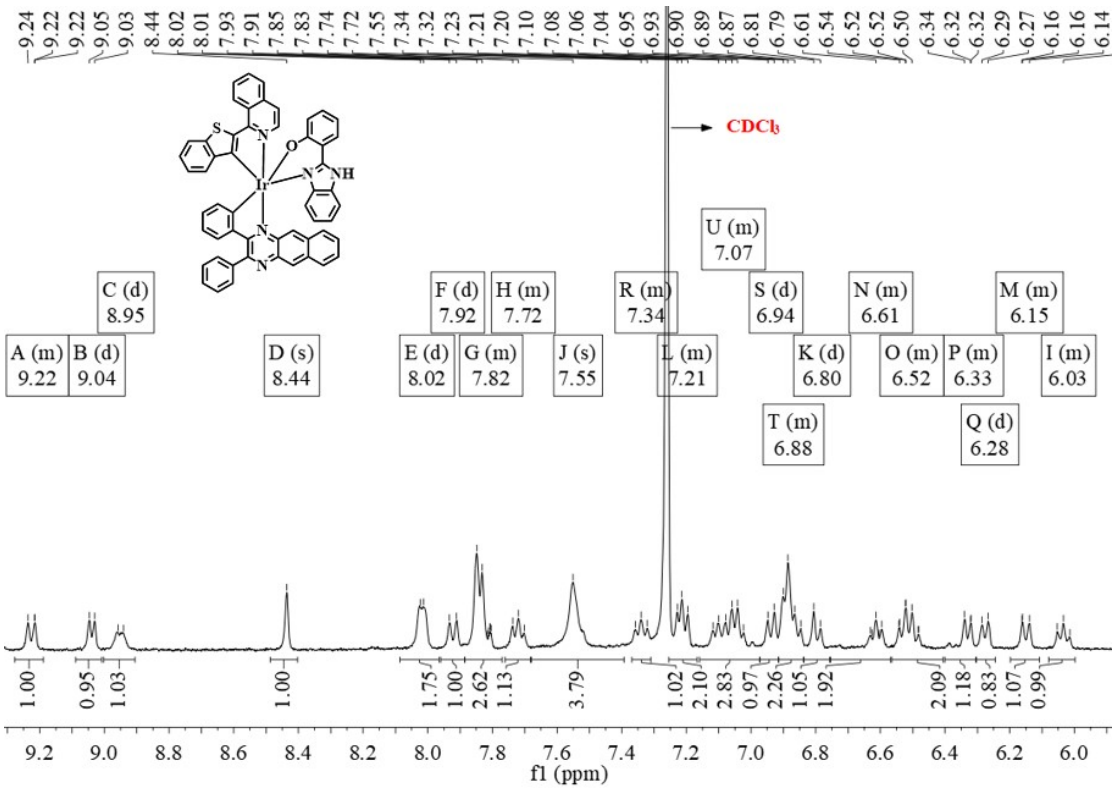

Figure S6. The thermogravimetric analysis (TG) curves for the Ir(III)-complexes [Ir(dpbq)$_2$(pbi)] (**1**) and [Ir(dpbq)(iqbt)(pbi)] (**2**), respectively.

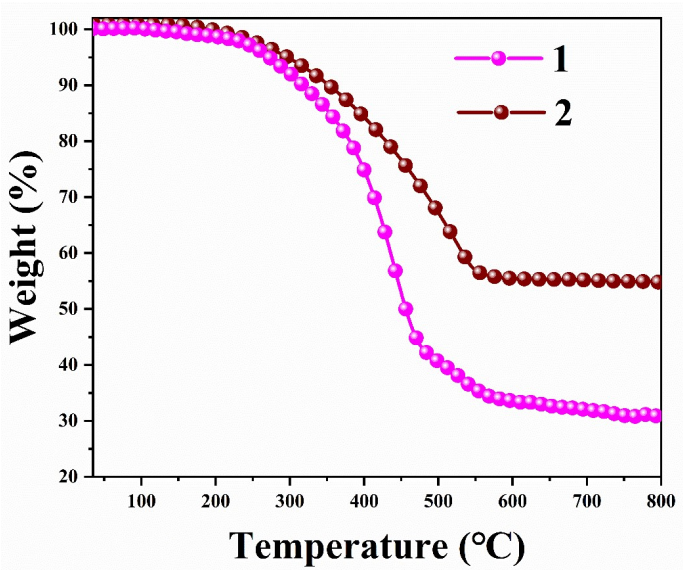

Figure S7. The normalized UV-visible absorption spectra of the **Hdpbq**-HC^N, **Hiqbt**-HC'^N′ and the N''^OH-**Hpbi** ligands in degassed CH_2Cl_2 solutions at room temperature, respectively.

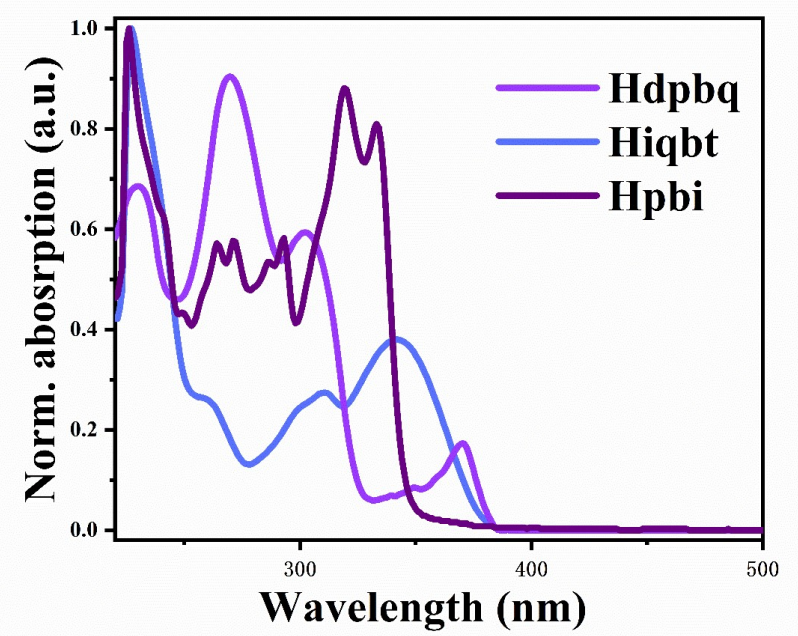

Figure S8. The normalized emission spectra of the **Hdpbq**-HC^N, **Hiqbt**-HC'^N′ and the N''^OH-**Hpbi** ligands in degassed CH_2Cl_2 solutions at room temperature, respectively.

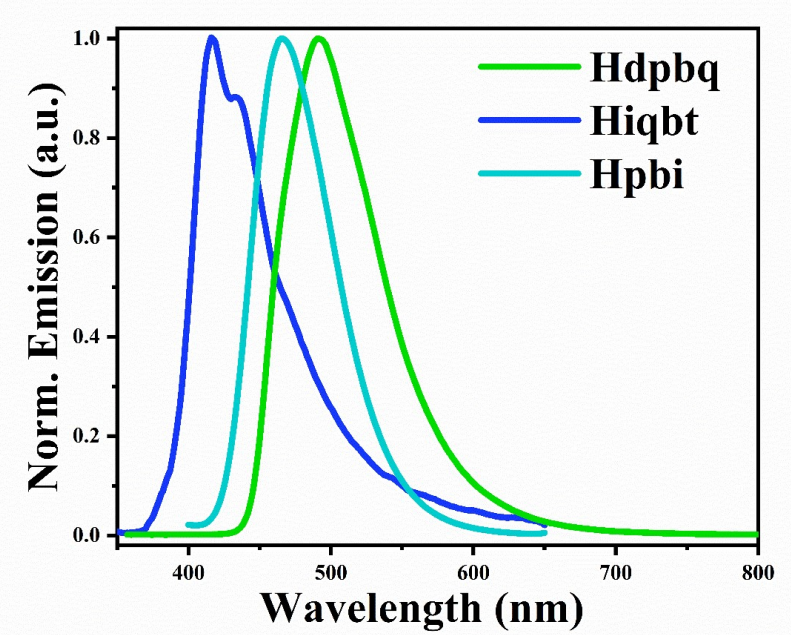

Figure S9. The cyclic voltammogram (CV) results of [Ir(dpbq)$_2$(pbi)] (**1**) and [Ir(dpbq)(iqbt)(pbi)] (**2**) recorded versus Fc^+/Fc in degassed MeCN solution at room temperature under a N_2 atmosphere (scan rate = 100 mV/s), respectively.

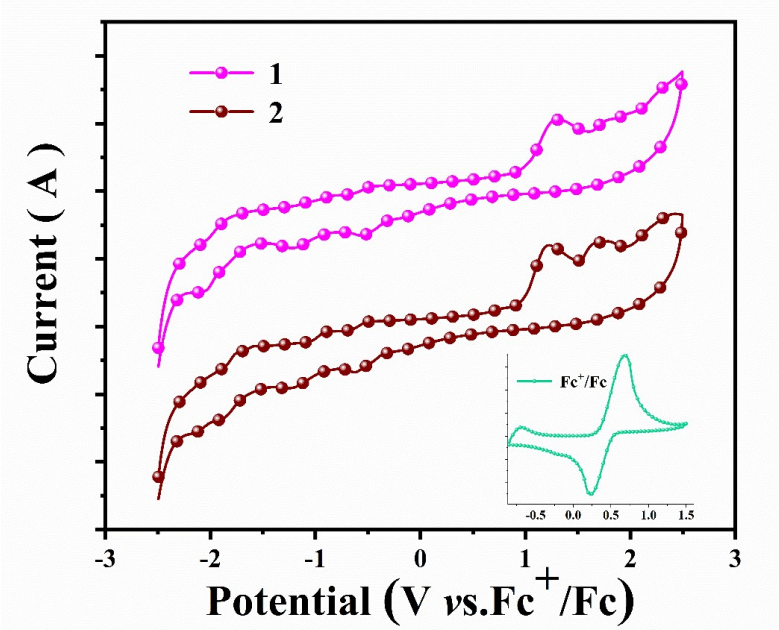

Figure S10. The electroluminescent spectra as a function of applied voltage (*V*) for the two **NIR-OLEDs-1/2** (2 wt%).